J. Fluid Mech. (2012), *vol.* 695, *pp.* 366–389.
doi:10.1017/jfm.2012.25

Anomalous dispersion in chemically heterogeneous media induced by long-range disorder correlation

D. Bolster[1]† **and M. Dentz**[2]

[1] Environmental Fluid Dynamics Laboratories, Department of Civil Engineering and Geological Sciences, University of Notre Dame, IN 46556, USA

[2] Institute of Environmental Assessment and Water Research (IDAEA), Spanish National Research Council (CSIC), 08034 Barcelona, Spain

(Received 17 April 2011; revised 30 December 2011; accepted 6 January 2012; first published online 13 February 2012)

We study transport in an idealized porous medium characterized by a spatially varying retardation factor, which models linear instantaneous chemical adsorption of a solute. Using a stochastic modelling approach, we study the impact of disorder correlation on the large-scale dispersion behaviour. We consider short, long-range and intermediate-range disorder correlations, and demonstrate that (truncated) power-law correlation causes anomalous dispersion, even in the presence of weak heterogeneity. We identify different preasymptotic and asymptotic regimes of anomalous dispersion that shed new light on the disorder and local-scale transport mechanisms leading to non-Fickian behaviour. The analytical results are complemented by numerical random walk particle tracking simulations, which are found to be in good agreement with the derived dispersion behaviour. We conclude the paper by deriving an effective transport equation for this system, which can be shown to be tied to the family of continuous-time random walk models.

Key words: geophysical and geological flows, mixing and dispersion, porous media

1. Introduction

Making accurate predictions of transport in the subsurface is notoriously difficult due to the heterogeneities that occur naturally in geological systems (Dagan 1984; Gelhar 1992; Tartakovsky & Winter 2008). Spatial heterogeneity of physical parameters is known to have a significant effect on transport on the large scale (Koch & Brady 1985, 1987; Dagan 1997). In particular, it is known that physical heterogeneity can lead to anomalous transport (e.g. Jones & Young 1994; Moroni & Cushman 2001; White & Nepf 2003), which means that spreading of the plume is not Fickian. Anomalous transport has been observed extensively in the laboratory (e.g. Silliman & Simpson 1987) and in the field (e.g. Gelhar, Welty & Rehfeldt 1992). The rate of spreading can be quantified by the temporal evolution of the spatial moments of the plume (e.g. Aris 1956; Gill & Sankarasubramanian 1970).

† Email address for correspondence: diogobolster@gmail.com

Studies of dispersion in moderately heterogeneous media typically result in Fickian-type spreading of plumes, suggesting that the non-Fickian behaviour observed in the laboratory (e.g. Levy & Berkowitz 2003) and in field experiments (e.g. Adams & Gelhar 1992) can be attributed to large degrees of heterogeneity. This certainly agrees with observations in highly heterogeneous systems (e.g. Adams & Gelhar 1992; Herrick *et al.* 2002; LeBorgne, Dentz & Carrera 2008), but does not explain observations in systems with relatively weak degrees of heterogeneity (e.g. Benson, Wheatcraft & Meerschaert 2000). In fact, anomalous transport can arise due to broad distributions of disorder point values as well as strong disorder correlation (e.g. Bouchaud & Georges 1990; Dentz & Castro 2009; Dentz & Bolster 2010). For transport in heterogeneous permeability fields, anomalous dispersion has been shown to occur in stratified media (e.g. Matheron & de Marsily 1980) as well as in media characterized by hierarchies of heterogeneity length scales of the random permeability field (e.g. Neuman 1990; Glimm & Sharp 1991; Dagan 1994; Rajaram & Gelhar 1995; Di Federico & Zhang 1999; Fiori 2001). Models that describe anomalous transport in highly heterogeneous porous media include multirate mass transfer (MRMT), continuous time random walk (CTRW) approaches and fractional advection–dispersion equations (e.g. Berkowitz *et al.* 2006; Neuman & Tartakovsky 2009). Such models describe anomalous transport caused by a broad heterogeneity distribution, which is mapped onto a distribution of characteristic transport time scales.

In this paper we study the impact of strong disorder correlation on large-scale anomalous dispersion. We consider an idealized heterogeneous porous medium that is characterized by spatial variability in linear equilibrium sorption–desorption properties as quantified by the retardation factor. The medium is assumed to be physically homogeneous even though in general there is a correlation between the retardation properties and the distribution of hydraulic conductivity in geological media (e.g. Bellin *et al.* 1993; Attinger *et al.* 1999; Dentz *et al.* 2000). As noted in Attinger *et al.* (1999), within the stochastic perturbative approach employed in this paper, the contributions to the dispersion coefficients due to different disorder sources simply add up. Here we focus on contributions due to heterogeneity in the retardation factor and disregard heterogeneity in hydraulic conductivity. Heterogeneity in the chemical properties of a medium, such as spatial variability of retardation, can have a significant impact on the transport properties of a dissolved substance (Chrysikopoulos, Kitanidis & Roberts 1990; Bellin *et al.* 1993; Miralles-Wilhelm & Gelhar 1996; Cvetkovic, Dagan & Cheng 1998; Attinger *et al.* 1999; Lenz & Kumar 2007; Dentz, Bolster & LeBorgne 2009; Dentz & Castro 2009). Retardation does not affect the fluid flow field, but plays a role on transport. Variations in the retardation coefficient affect solute spreading (e.g. Bellin *et al.* 1993; Attinger *et al.* 1999) and can lead to local accumulation and release of the solute (e.g. Sanchez-Vila & Bolster 2009). The quantification of the impact of heterogeneity on sorption–desorption reactions plays a key role in the fate of many natural and anthropogenic contaminants such as organic compounds, heavy metals, transition metals and radionuclides (e.g. Grathwohl 1998).

A systematic method to capture the impact of heterogeneity in retardation on large-scale dispersion is a stochastic modelling approach (e.g. Chrysikopoulos *et al.* 1990; Bellin *et al.* 1993; Miralles-Wilhelm & Gelhar 1996; Andricevic & Cvetkovic 1998; Attinger *et al.* 1999; Rubin *et al.* 1999; Dentz & Castro 2009), which models spatially fluctuating retardation properties as statistically stationary random fields. The effective transport behaviour is derived by appropriately averaging over the ensemble of all possible disorder realizations. Large-scale solute transport is quantified by the evolution of effective and ensemble dispersion coefficients (e.g. Attinger *et al.*

1999), which are evaluated using a second-order perturbation theory approach in the fluctuations of the random retardation factor. While Attinger *et al.* (1999) analysed the behaviour of the ensemble and effective dispersion coefficient for short-range disorder correlation, here our focus is on the impact of long-range correlation of the retardation factor on anomalous large-scale dispersion. Furthermore, within this stochastic approach, we derive a large-scale transport equation for the average solute concentration, whose properties are studied using second-order perturbation theory. Discussions of possible limitations of perturbation methods for transport in porous media can be found in Bellin, Salandin & Rinaldo (1992), Trefry, Ruan & McLaughlin (2003) and Jarman & Tartakovsky (2008).

The paper is organized as follows. Section 2 presents the heterogeneous system that we study in this work. In § 3 we analytically develop and calculate the dispersion coefficients associated with this system. In § 4, for validation purposes, we compare our analytical predictions to the results of efficient numerical random walk simulations. In § 5 we develop the effective upscaled CTRW model, and we conclude with a discussion in § 6.

2. Model

2.1. *Local-scale transport description*

On a local scale, the transport of a solute with instantaneous adsorption in a chemically heterogeneous medium for $t \geqslant 0$ can be described by (Attinger *et al.* 1999)

$$\frac{\partial}{\partial t}[R(\boldsymbol{x})g(\boldsymbol{x},t)] + u\frac{\partial}{\partial x_1}g(\boldsymbol{x},t) - \boldsymbol{\nabla}\cdot[\boldsymbol{D}\cdot\boldsymbol{\nabla}g(\boldsymbol{x},t)] = 0, \tag{2.1}$$

where $g(\boldsymbol{x},t)$ is the concentration of mobile solute, and u and $\boldsymbol{D}$ are the constant local flow (filtration) velocity and the constant dispersion tensor, respectively. Without loss of generality, the flow velocity is aligned with the 1-direction of the coordinate system. The dispersion tensor is assumed to be diagonal, $D_{ij} = \delta_{ij}D_{ii}$. The spatially varying retardation factor $R(\boldsymbol{x})$ accounts for variation in the local chemical adsorption properties. While this model is motivated by porous media, it can in principle represent transport in any other system with spatially variable retardation. In this study the retardation coefficient is given by

$$R(\boldsymbol{x}) = 1 + k_d(\boldsymbol{x}), \tag{2.2}$$

where the coefficient $k_d(\boldsymbol{x})$ relates the mobile concentration $g(\boldsymbol{x},t)$ to the concentration $g_{ads}(\boldsymbol{x},t)$ of adsorbed solute:

$$g_{ads}(\boldsymbol{x},t) = k_d(\boldsymbol{x})g(\boldsymbol{x},t). \tag{2.3}$$

As boundary conditions for the mobile concentration, we assume vanishing $g(\boldsymbol{x},t)$ at infinity. The initial condition for the mobile concentration $g(\boldsymbol{x},t)$ is a point source given by $g(\boldsymbol{x},t=0) = R^{-1}(0)\delta(\boldsymbol{x})$. Thus, the total concentration

$$c(\boldsymbol{x},t) = R(\boldsymbol{x})g(\boldsymbol{x},t) \tag{2.4}$$

also has a point-source initial condition $c(\boldsymbol{x},t=0) = \delta(\boldsymbol{x})$.

2.2. *Stochastic model and ensemble average*

The influence of spatial fluctuations of the retardation factor $R(\boldsymbol{x})$ is addressed in a stochastic modelling framework. The spatially fluctuating retardation factor $R(\boldsymbol{x})$ is assumed to be a translationally invariant random field. Thus, $R(\boldsymbol{x})$ in a given medium

represents a typical realization of an ensemble of the corresponding random fields. The translational invariance of $R(\boldsymbol{x})$ implies that $\overline{R(\boldsymbol{x})} = \overline{R}$ is constant, where the overbar in the following denotes the ensemble average, which is the average over all possible realizations of the random space function $k_d(\boldsymbol{x})$. Here, the spatially varying distribution coefficient $k_d(\boldsymbol{x})$ is modelled as a lognormally distributed random field (e.g. Bellin *et al.* 1993),

$$k_d(\boldsymbol{x}) = K_d \exp[\mu(\boldsymbol{x})], \tag{2.5}$$

where K_d denotes the geometric mean of $k_d(\boldsymbol{x})$, and $\mu(\boldsymbol{x})$ is a Gaussian-distributed random field with zero mean and correlation function

$$\overline{\mu(\boldsymbol{x})\mu(\boldsymbol{x}')} = \sigma^2_{\mu\mu} C_{\mu\mu}(\boldsymbol{x} - \boldsymbol{x}'), \tag{2.6}$$

with $C_{\mu\mu}(0) = 1$ and $\sigma^2_{\mu\mu}$ the variance of $\mu(\boldsymbol{x})$. The ensemble mean retardation factor is then given by

$$\overline{R(\boldsymbol{x})} = 1 + K_d \exp\left(\frac{\sigma^2_{\mu\mu}}{2}\right). \tag{2.7}$$

We split $R(\boldsymbol{x})$ into its constant mean value and fluctuations about it,

$$R(\boldsymbol{x}) = \overline{R}[1 + r(\boldsymbol{x})], \tag{2.8}$$

where $r(\boldsymbol{x})$ is given by

$$r(\boldsymbol{x}) = \frac{K_d}{1 + K_d \exp(\sigma^2_{\mu\mu}/2)} \{\exp[\mu(\boldsymbol{x})] - \exp(\sigma^2_{\mu\mu}/2)\}. \tag{2.9}$$

The mean $\overline{r(\boldsymbol{x})} = 0$ by definition. The autocorrelation function of $r(\boldsymbol{x})$ is given by

$$\overline{r(\boldsymbol{x})r(\boldsymbol{x}')} = C_{rr}(\boldsymbol{x} - \boldsymbol{x}') = q\{\exp[\sigma^2_{\mu\mu} C_{\mu\mu}(\boldsymbol{x} - \boldsymbol{x}')] - 1\}, \tag{2.10}$$

where q is defined by (e.g. Attinger *et al.* 1999)

$$q = \frac{K_d^2 \exp(\sigma^2_{\mu\mu})}{[1 + K_d \exp(\sigma^2_{\mu\mu}/2)]^2} = \frac{\overline{R^2} - \overline{R}^2}{\overline{R}^2}. \tag{2.11}$$

In the following, we approximate $C_{rr}(\boldsymbol{x})$ to first order in $\sigma^2_{\mu\mu}$ as

$$C_{rr}(\boldsymbol{x}) = \sigma^2 C_{\mu\mu}(\boldsymbol{x}), \quad \sigma^2 = \frac{\sigma^2_{\mu\mu} K_d^2}{(1 + K_d)^2}. \tag{2.12}$$

2.3. *Dimensionless form of the governing equations*

We now introduce the following dimensionless variables

$$x_i = \ell \hat{x}_i, \quad t = \tau_u \hat{t}, \tag{2.13}$$

where ℓ is a characteristic heterogeneity length scale and the advection time scale is $\tau_u = \overline{R}\ell/u$. The concentrations are rescaled as $g(\boldsymbol{x}, t) = \overline{R}^{-1} \ell^{-d} \hat{g}(\boldsymbol{x}, t)$ and $c(\boldsymbol{x}, t) = \ell^{-d} \hat{c}(\boldsymbol{x}, t)$, in which d denotes the dimensionality of space. Using these definitions, (2.1) can be written in dimensionless form as

$$\frac{\partial \hat{g}(\hat{\boldsymbol{x}}, \hat{t})}{\partial \hat{t}} + \frac{\partial \hat{g}(\hat{\boldsymbol{x}}, \hat{t})}{\partial \hat{x}_1} - \hat{\boldsymbol{\nabla}} \cdot [\hat{\boldsymbol{D}} \cdot \hat{\boldsymbol{\nabla}} \hat{g}(\hat{\boldsymbol{x}}, \hat{t})] = -r(\hat{\boldsymbol{x}}) \frac{\partial \hat{g}(\hat{\boldsymbol{x}}, \hat{t})}{\partial \hat{t}}, \tag{2.14}$$

where $\hat{\boldsymbol{D}} = \boldsymbol{D}/(u\ell)$ is the dispersion tensor in dimensionless form. The initial condition for $\hat{g}(\hat{\boldsymbol{x}}, t)$ is $\hat{g}(\hat{\boldsymbol{x}}, t = 0) = [1 + r(\boldsymbol{0})]^{-1}\, \delta(\hat{\boldsymbol{x}})$. Relation (2.4) between total and mobile concentration gives

$$\hat{c}(\hat{\boldsymbol{x}}, \hat{t}) = [1 + r(\hat{\boldsymbol{x}})]\hat{g}(\hat{\boldsymbol{x}}, \hat{t}). \tag{2.15}$$

For simplicity of notation, from here on, we drop the hats, and unless otherwise indicated, all quantities are dimensionless.

2.4. *Integral equation and perturbation series*

For technical convenience, we perform a Fourier transform of the governing equations. The Fourier transform of a function $\varphi(x)$ and its back-transform here are defined by

$$\widetilde{\varphi}(\boldsymbol{k}) = \int \mathrm{d}\boldsymbol{x} \exp(\mathrm{i}\boldsymbol{k} \cdot \boldsymbol{x})\varphi(\boldsymbol{x}), \tag{2.16}$$

$$\varphi(\boldsymbol{x}) = \int_k \exp(-\mathrm{i}\boldsymbol{k} \cdot \boldsymbol{x})\widetilde{\varphi}(\boldsymbol{k}), \tag{2.17}$$

in which the tilde denotes Fourier-transformed quantities, and the wavevector is denoted by $\boldsymbol{k}$. Here and in the following we use the short-hand notation

$$\int_k \cdots \equiv \int \frac{\mathrm{d}\boldsymbol{k}}{(2\pi)^d}, \tag{2.18}$$

in which the superscript d denotes the dimensionality of space. Thus, the Fourier transform of (2.14) yields

$$\frac{\partial}{\partial t}\widetilde{g}(\boldsymbol{k}, t) - [\mathrm{i}k_1 - \boldsymbol{k} \cdot (\boldsymbol{D} \cdot \boldsymbol{k})]\widetilde{g}(\boldsymbol{k}, t) = -\int_{k'} \widetilde{r}(\boldsymbol{k}')\frac{\partial}{\partial t}\widetilde{g}(\boldsymbol{k} - \boldsymbol{k}', t). \tag{2.19}$$

Let us define $\widetilde{g}_0(\boldsymbol{k}, t)$ as the solution to (2.19) with $\widetilde{r}(\boldsymbol{k}') = 0$ and initial condition $\widetilde{g}(\boldsymbol{k}, t = 0) = 1$, that is,

$$\widetilde{g}_0(\boldsymbol{k}, t) = \exp(-\boldsymbol{k} \cdot \boldsymbol{D} \cdot \boldsymbol{k}t + \mathrm{i}k_1 t). \tag{2.20}$$

Convolving (2.19) with $\widetilde{g}_0(\boldsymbol{k}, t)$ and performing a partial integration, we obtain

$$\widetilde{g}(\boldsymbol{k}, t) = \frac{\widetilde{g}_0(\boldsymbol{k}, t)}{1 + r(\boldsymbol{0})} - \int_0^t \mathrm{d}t'\, \widetilde{g}_0(\boldsymbol{k}, t - t') \int_{k'} \widetilde{r}(\boldsymbol{k}')\frac{\partial}{\partial t'}\widetilde{g}(\boldsymbol{k} - \boldsymbol{k}', t'). \tag{2.21}$$

Using relation (2.15) between the total and mobile concentrations in (2.21) and integrating by parts, the total concentration is

$$\widetilde{c}(\boldsymbol{k}, t) = \widetilde{g}_0(\boldsymbol{k}, t) + \int_0^t \mathrm{d}t' \frac{\partial}{\partial t'}\widetilde{g}_0(\boldsymbol{k}, t - t') \int_{k'} \widetilde{r}(\boldsymbol{k}')\widetilde{g}(\boldsymbol{k} - \boldsymbol{k}', t'). \tag{2.22}$$

By iteration of integral equation (2.21) we obtain

$$\begin{aligned}\widetilde{g}(\boldsymbol{k}, t) = \widetilde{g}_0(\boldsymbol{k}, t) &- \int_{k'} \widetilde{r}(\boldsymbol{k}')\widetilde{g}_0(\boldsymbol{k}, t) \\ &- \int_0^t \mathrm{d}t'\, \widetilde{g}_0(\boldsymbol{k}, t - t') \int_{k'} \widetilde{r}(\boldsymbol{k}')\frac{\partial}{\partial t'}\widetilde{g}_0(\boldsymbol{k} - \boldsymbol{k}', t') + \cdots,\end{aligned} \tag{2.23}$$

up to first order in $\widetilde{r}(\boldsymbol{k})$. The dots denote sub-leading contributions. A perturbation expression for $\widetilde{c}(\boldsymbol{k}, t)$ up to second order in $\widetilde{r}(\boldsymbol{k})$ is obtained by inserting (2.23) into the

right-hand side of (2.22),

$$\widetilde{c}(\boldsymbol{k},t)=\widetilde{g}_0(\boldsymbol{k},t)+\widetilde{c}_1(\boldsymbol{k},t)+\widetilde{c}_2(\boldsymbol{k},t)+\cdots, \tag{2.24}$$

where

$$\widetilde{c}_1(\boldsymbol{k},t)=\int_0^t \mathrm{d}t'\,\frac{\partial}{\partial t'}\widetilde{g}_0(\boldsymbol{k},t-t')\int_{k'}\widetilde{r}(\boldsymbol{k}')\widetilde{g}_0(\boldsymbol{k}-\boldsymbol{k}',t') \tag{2.25}$$

$$\begin{aligned}\widetilde{c}_2(\boldsymbol{k},t)=&-\int_0^t \mathrm{d}t'\,\frac{\partial}{\partial t'}\widetilde{g}_0(\boldsymbol{k},t-t')\int_{k'}\int_{k''}\widetilde{r}(\boldsymbol{k}')\widetilde{r}(\boldsymbol{k}'')\widetilde{g}_0(\boldsymbol{k}-\boldsymbol{k}',t')\\&-\int_0^t \mathrm{d}t'\,\frac{\partial}{\partial t'}\widetilde{g}_0(\boldsymbol{k},t-t')\int_0^{t'}\mathrm{d}t''\int_{k'}\int_{k''}\widetilde{r}(\boldsymbol{k}')\widetilde{g}_0(\boldsymbol{k}-\boldsymbol{k}',t'-t'')\\&\times\widetilde{r}(\boldsymbol{k}'')\frac{\partial}{\partial t''}\widetilde{g}_0(\boldsymbol{k}-\boldsymbol{k}'-\boldsymbol{k}'',t'')+\cdots.\end{aligned} \tag{2.26}$$

The dots denote sub-leading contributions.

3. Dispersion coefficients

In this section we derive perturbation expressions for the effective and ensemble dispersion coefficients of the total concentration distribution $c(\boldsymbol{x},t)$. The effective dispersion coefficients are defined as

$$D_{ij}^{eff}(t)=-\frac{1}{2}\frac{\partial}{\partial t}\frac{\partial^2}{\partial k_i k_j}\overline{\ln[\widetilde{c}(\boldsymbol{k},t)]}|_{\boldsymbol{k}=0}, \tag{3.1}$$

i.e. they are derived from the ensemble-averaged second centred moment. Similarly, we can define the ensemble dispersion coefficients with the second centred moment of the ensemble-averaged total concentration distribution, i.e.

$$D_{ij}^{ens}(t)=-\frac{1}{2}\frac{\partial}{\partial t}\frac{\partial^2}{\partial k_i k_j}\ln[\overline{\widetilde{c}(\boldsymbol{k},t)}]|_{\boldsymbol{k}=0}. \tag{3.2}$$

Physically the difference between these two dispersion coefficients can be interpreted as follows (e.g. Batchelor 1949; Kitanidis 1988; Dagan 1990, 1991; Attinger *et al.* 1999; Dentz *et al.* 2000; Fiori 2001; Lawrence & Rubin 2007; de Barros & Rubin 2011). The effective dispersion coefficient D_{ij}^{eff} represents the average value of the dispersion coefficients measured over several realizations, while the ensemble dispersion coefficient D_{ij}^{ens} represents the dispersion coefficients calculated from the concentration averaged over all realizations.

The generating function $\overline{\ln[\widetilde{c}(\boldsymbol{k},t)]}$ for the effective dispersion coefficients is determined within second-order perturbation theory by inserting perturbation expansion (2.24) into $\ln[\widetilde{c}(\boldsymbol{k},t)]$,

$$\ln[\widetilde{c}(\boldsymbol{k},t)]=\ln[\widetilde{g}_0(\boldsymbol{k},t)]+\ln[1+\widetilde{g}_0(\boldsymbol{k},t)^{-1}\widetilde{c}_1(\boldsymbol{k},t)+\widetilde{g}_0(\boldsymbol{k},t)^{-1}\widetilde{c}_2(\boldsymbol{k},t)+\cdots]. \tag{3.3}$$

Expanding the second term on the right-hand side by using $\ln(1+x)=x-x^2/2+\cdots$ gives

$$\begin{aligned}\ln[\widetilde{c}(\boldsymbol{k},t)]=&\ln[\widetilde{g}_0(\boldsymbol{k},t)]+\widetilde{g}_0(\boldsymbol{k},t)^{-1}\widetilde{c}_1(\boldsymbol{k},t)+\widetilde{g}_0(\boldsymbol{k},t)^{-1}\widetilde{c}_2(\boldsymbol{k},t)\\&-\tfrac{1}{2}\widetilde{g}_0(\boldsymbol{k},t)^{-2}\widetilde{c}_1^2(\boldsymbol{k},t)+\cdots.\end{aligned} \tag{3.4}$$

Inserting expressions (2.25) and (2.26) and performing the ensemble average results in

$$\begin{aligned}\overline{\ln[\widetilde{c}(\boldsymbol{k},t)]} = \ln[\widetilde{g}_0(\boldsymbol{k},t)] &- \widetilde{g}_0^{-1}(\boldsymbol{k},t)\int_0^t \mathrm{d}t' \int_{k'} \frac{\partial}{\partial t'}\widetilde{g}_0(\boldsymbol{k},t-t')\widetilde{C}_{rr}(\boldsymbol{k}')\widetilde{g}_0(\boldsymbol{k}-\boldsymbol{k}',t') \\ &- \widetilde{g}_0^{-1}(\boldsymbol{k},t)\int_0^t \mathrm{d}t' \int_0^{t'} \mathrm{d}t'' \int_{k'} \frac{\partial}{\partial t'}\widetilde{g}_0(\boldsymbol{k},t-t')\widetilde{C}_{rr}(\boldsymbol{k}') \\ &\quad \times \widetilde{g}_0(\boldsymbol{k}-\boldsymbol{k}',t'-t'')\frac{\partial}{\partial t''}\widetilde{g}_0(\boldsymbol{k},t'') \\ &- \frac{1}{2}\widetilde{g}_0^{-2}(\boldsymbol{k},t)\int_0^t \mathrm{d}t' \int_0^{t'} \mathrm{d}t'' \int_{k'} \frac{\partial}{\partial t'}\widetilde{g}_0(\boldsymbol{k},t-t')\widetilde{C}_{rr}(\boldsymbol{k}')\widetilde{g}_0(\boldsymbol{k}-\boldsymbol{k}',t') \\ &\quad \times \frac{\partial}{\partial t''}\widetilde{g}_0(\boldsymbol{k},t-t'')\widetilde{g}_0(\boldsymbol{k}+\boldsymbol{k}',t'') + \cdots . \end{aligned} \tag{3.5}$$

In order to derive the generating function $\ln[\overline{\widetilde{c}(\boldsymbol{k},t)}]$, we insert the average of (2.24), which gives

$$\ln[\overline{\widetilde{c}(\boldsymbol{k},t)}] = \ln[\widetilde{g}_0(\boldsymbol{k},t)] + \ln[1+\widetilde{g}_0(\boldsymbol{k},t)^{-1}\,\overline{\widetilde{c}_2(\boldsymbol{k},t)} + \cdots]. \tag{3.6}$$

Expanding the second term on the right-hand side using $\ln[1+x] = x - \cdots$ yields

$$\ln[\overline{\widetilde{c}(\boldsymbol{k},t)}] = \ln[\widetilde{g}_0(\boldsymbol{k},t)] + \widetilde{g}_0(\boldsymbol{k},t)^{-1}\,\overline{\widetilde{c}_2(\boldsymbol{k},t)} + \cdots . \tag{3.7}$$

Inserting (2.26) for $\widetilde{c}_2(\boldsymbol{k},t)$ gives

$$\begin{aligned}\ln[\overline{\widetilde{c}(\boldsymbol{k},t)}] = \ln[\widetilde{g}_0(\boldsymbol{k},t)] &- \widetilde{g}_0^{-1}(\boldsymbol{k},t)\int_0^t \mathrm{d}t' \int_{k'} \frac{\partial}{\partial t'}\widetilde{g}_0(\boldsymbol{k},t-t')\widetilde{C}_{rr}(\boldsymbol{k}')\widetilde{g}_0(\boldsymbol{k}-\boldsymbol{k}',t') \\ &- \widetilde{g}_0^{-1}(\boldsymbol{k},t)\int_0^t \mathrm{d}t' \int_0^{t'} \mathrm{d}t'' \int_{k'} \frac{\partial}{\partial t'}\widetilde{g}_0(\boldsymbol{k},t-t')\widetilde{C}_{rr}(\boldsymbol{k}') \\ &\quad \times \widetilde{g}_0(\boldsymbol{k}-\boldsymbol{k}',t'-t'')\frac{\partial}{\partial t''}\widetilde{g}_0(\boldsymbol{k},t'') + \cdots . \end{aligned} \tag{3.8}$$

Now, inserting (3.8) and (3.5) into (3.2) and (3.1), respectively, the dispersion coefficients are given by

$$\begin{aligned} D_{ij}^{ens}(t) = D_{ij} &+ \delta_{i1}\delta_{j1}\int_0^t \mathrm{d}t' \int_{k'} \widetilde{g}_0(\boldsymbol{k}',t')\widetilde{C}_{rr}(\boldsymbol{k}') \\ &+ \int_{k'} \widetilde{C}_{rr}(\boldsymbol{k}')(D_{ij} - \mathrm{i}\delta_{j1}D_{im}k'_m t' - \mathrm{i}\delta_{i1}D_{jm}k'_m t')\widetilde{g}_0(-\boldsymbol{k}',t), \end{aligned} \tag{3.9}$$

$$D_{ij}^{eff}(t) = D_{ij}^{ens}(t) - \delta_{i1}\delta_{j1}\int_0^t \mathrm{d}t' \int_{k'} \widetilde{g}_0(\boldsymbol{k}',t)\widetilde{C}_{rr}(\boldsymbol{k}')\widetilde{g}_0(-\boldsymbol{k}',t'). \tag{3.10}$$

For the following investigation we focus on advection-dominated scenarios, which are characterized by $D_{ij} \ll 1$. Thus, we will disregard the third contribution on the right-hand side of (3.9). In this scenario, the dispersion coefficients perpendicular to the mean flow direction are sub-leading. Thus, we focus only on the dispersion coefficients in the longitudinal direction.

In the limiting case of $\boldsymbol{D} \equiv \boldsymbol{0}$, the effective dispersion coefficients are by definition identically equal to zero (e.g. Attinger *et al.* 1999) and the ensemble dispersion

coefficients are given by

$$D_{ij}^{ens}(t) = \delta_{i1}\delta_{j1}\int_0^t \mathrm{d}t'\, C_{rr}(t'), \tag{3.11}$$

where $C_{rr}(t) = C_{rr}(\boldsymbol{x})|_{x_1=t,\, x_2,\ldots,x_d=0}$.

3.1. *Correlation function*

In the following we employ the first-order approximation (2.12) for the correlation function of the normalized retardation fluctuations in terms of $C_{\mu\mu}(\boldsymbol{x})$. We assume that $C_{\mu\mu}(\boldsymbol{x})$ can be factorized such that

$$C_{\mu\mu}(\boldsymbol{x}) = C_1(x_1)\cdots C_d(x_d), \tag{3.12}$$

i.e. correlations in each principal direction are independent of the correlations in the other principal directions. The Fourier transform of (3.12) is given by

$$\widetilde{C}_{\mu\mu}(\boldsymbol{k}) = \widetilde{C}_1(k_1)\cdots\widetilde{C}_d(k_d). \tag{3.13}$$

We assume that all correlation functions are even. Specifically, for correlations perpendicular to the direction of flow, $C_i(x_i)$ $(i \neq 1)$, we assume short-range correlations that we model using Gaussian-shaped functions

$$C_i(x_i) = \exp\left(-\frac{x_i^2}{2}\right). \tag{3.14}$$

For simplicity, we assume that the correlation lengths in all different directions are the same and thus equal to 1. The Fourier transform of (3.14) is given by

$$\widetilde{C}_i(k_i) = \sqrt{2\pi}\exp\left(-\frac{k_i^2}{2}\right). \tag{3.15}$$

Inserting expressions (3.13) and (3.15) for the Fourier transform of the correlation function and (2.20) for $\widetilde{g}_0(\boldsymbol{k}, t)$ into expressions (3.9) and (3.10) for the longitudinal ensemble and effective dispersion coefficients, respectively, we obtain

$$\begin{aligned} D_{11}^{ens}(t) = D_{11} + \sigma^2 \int_0^t \mathrm{d}t' \prod_{i=2}^{d} (1 + 2D_{ii}t')^{-1/2}, \\ \times \int_{-\infty}^{\infty} \frac{\mathrm{d}k_1}{2\pi} \exp(-k_1^2 D_{11}t' - \mathrm{i}k_1 t')\widetilde{C}_1(k_1) \end{aligned} \tag{3.16}$$

$$\begin{aligned} D_{11}^{eff}(t) = D_{11}^{ens}(t) - \sigma^2 \int_0^t \mathrm{d}t' \prod_{i=2}^{d} (1 - 2D_{ii}t' + 4D_{ii}t)^{-1/2} \\ \times \int_{-\infty}^{\infty} \frac{\mathrm{d}k_1}{2\pi} \exp(-D_{11}k_1^2(2t - t') - \mathrm{i}k_1 t')\widetilde{C}_1(k_1). \end{aligned} \tag{3.17}$$

In the following analysis, we focus on cases for which $D_{ii} \ll 1$, which implies that the advection time scale τ_u is much smaller than the dispersion time scale $\tau_{D_i} = 1/D_{ii}$ for $i = 1, \ldots, d$. Note that, in porous media, the dispersion coefficient in the flow direction can be an order of magnitude larger than the transverse dispersion coefficients. However, the physical mechanism that enables the solute to sample the medium heterogeneity is transverse dispersion; longitudinal dispersion plays only a subordinate role. Thus, we can disregard D_{11} in approximations (3.16) and (3.17),

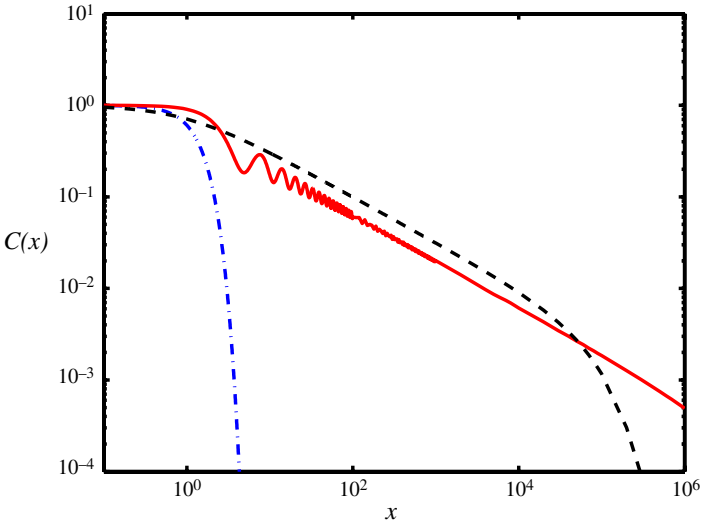

FIGURE 1. (Colour online available at journals.cambridge.org/flm) Gaussian (blue dash-dot), power law with $\beta = 3/2$ (red solid line) and truncated power law with $\beta = 3/2$ and cutoff length $l_c = 10^5$ (black dashed line).

which gives the approximations

$$D_{11}^{ens}(t) = \sigma^2 \int_0^t \mathrm{d}t' \prod_{i=2}^{d} (1 + 2D_{ii}t')^{-1/2} \int_{-\infty}^{\infty} \frac{\mathrm{d}k_1}{2\pi} \exp(-\mathrm{i}k_1 t') \widetilde{C}_1(k_1) + \cdots$$
$$= \sigma^2 \int_0^t \mathrm{d}t' C_1(t') \prod_{i=2}^{d} (1 + 2D_{ii}t')^{-1/2} + \cdots, \tag{3.18}$$

$$D_{11}^{eff}(t) = D_{11}^{ens}(t) - \sigma^2 \int_0^t \mathrm{d}t' \prod_{i=2}^{d} (1 - 2D_{ii}t' + 4D_{ii}t)^{-1/2}$$
$$\times \int_{-\infty}^{\infty} \frac{\mathrm{d}k_1}{2\pi} \exp(-\mathrm{i}k_1 t') \widetilde{C}_1(k_1) \cdots$$
$$= D_{11}^{ens}(t) - \sigma^2 \int_0^t \mathrm{d}t' C_1(t') \prod_{i=2}^{d} (1 - 2D_{ii}t' + 4D_{ii}t)^{-1/2} + \cdots, \tag{3.19}$$

where the dots denote sub-leading contributions. Using these expressions, in the following we study the dispersion coefficients for three different longitudinal correlation functions. In particular, we focus on the impact of correlations over short (Gaussian, blue), long (power law, red) and intermediate (truncated power law, black) distances. Examples of the three types of correlation function used in this paper are shown in figure 1.

3.1.1. *Short-range correlation*

To begin, we consider a short-range autocorrelation function in the direction of flow. To do so, we will use a Gaussian correlation function (like the transverse correlation functions) defined in (3.14) and (3.15), i.e.

$$C_1(x_1) = \exp\left(-\frac{x_1^2}{2}\right), \quad \widetilde{C}_1(k_1) = \sqrt{2\pi} \exp\left(-\frac{k_1^2}{2}\right). \tag{3.20}$$

Note that Attinger *et al.* (1999) studied this case in detail for the effective and ensemble dispersion coefficients derived from the mobile concentration $g(\boldsymbol{x}, t)$. Here we consider the moments of the total concentration $c(\boldsymbol{x}, t)$, whose behaviour is basically the same as the one found in Attinger *et al.* (1999). We discuss this short-range scenario for completeness and comparison to the long-range correlation scenarios here.

Using (3.20) in (3.18) and (3.19), the longitudinal ensemble and effective dispersion coefficients are given by

$$D_{11}^{ens}(t) = \sigma^2 \int_0^t \mathrm{d}t' \exp\left(-\frac{t'^2}{2}\right) \prod_{i=2}^{d} (1 + 2D_{ii}t')^{-1/2} + \cdots, \tag{3.21}$$

$$D_{11}^{eff}(t) = D_{11}^{ens}(t) - \sigma^2 \int_0^t \mathrm{d}t' \exp\left(-\frac{t'^2}{2}\right) \prod_{i=2}^{d} (1 - 2D_{ii}t' + 4D_{ii}t)^{-1/2} + \cdots, \tag{3.22}$$

where the dots denote sub-leading contributions. For times small compared to the advection time scale $\tau_u = 1$, $t \ll \tau_u$, the effective dispersion coefficient (3.17) is of the order of D_{11}. The ensemble dispersion coefficient (3.16) shows ballistic behaviour,

$$D_{11}^{ens}(t) = \sigma^2 t + \cdots, \tag{3.23}$$

where the dots denote sub-leading contributions of $O(t^2)$. In the intermediate time regime, which lies between the advection time scale τ_u and the smallest of the dispersion time scales $\tau_{D_i} = 1/D_{ii}$ (for $i = 2, \ldots, d$), the ensemble and effective dispersion coefficients can be approximated by

$$D_{11}^{ens}(t) = \sigma^2 \sqrt{\frac{\pi}{2}} + \cdots, \tag{3.24}$$

$$D_{11}^{eff}(t) = \sigma^2 \sqrt{\frac{\pi}{2}} \left[1 - \prod_{i=2}^{d} (1 + 4D_{ii}t)^{-1/2}\right] + \cdots. \tag{3.25}$$

In the asymptotic time regime, which is defined by the largest of the dispersion time scales, the ensemble and effective dispersion coefficients converge to the same asymptotic value. This is to be expected from generalized Taylor theory, which predicts a single asymptotic dispersion coefficient (e.g. Brenner 1980; Edwards & Brenner 1993; Latini & Bernoff 2001; Lunati, Attinger & Kinzelbach 2002; Bolster, Dentz & LeBorgne 2009; de Barros & Rubin 2011). Note that the effective dispersion coefficient $D_{11}^{eff}(t)$ evolves on the diffusion time scale, while $D_{11}^{ens}(t)$ evolves on the advection scale. An example illustrating this predicted behaviour for ensemble and effective dispersion coefficients is shown in figure 2.

3.1.2. *Power-law correlation*

As highlighted in the Introduction, one of the goals of this work is to illustrate the influence of long-range correlation on dispersion. Therefore, next we consider a correlation function with power-law behaviour. Such a correlation function reflects correlation over very long ranges. To this end we use

$$C_1(x_1) = (\beta - 1) \int_0^1 \mathrm{d}k_1 \cos(k_1 x_1) k_1^{\beta - 2}, \tag{3.26}$$

for $1 < \beta < 2$. For distances of the order of or smaller than 1, the medium appears homogeneous in the 1-direction and the correlation function has an approximately

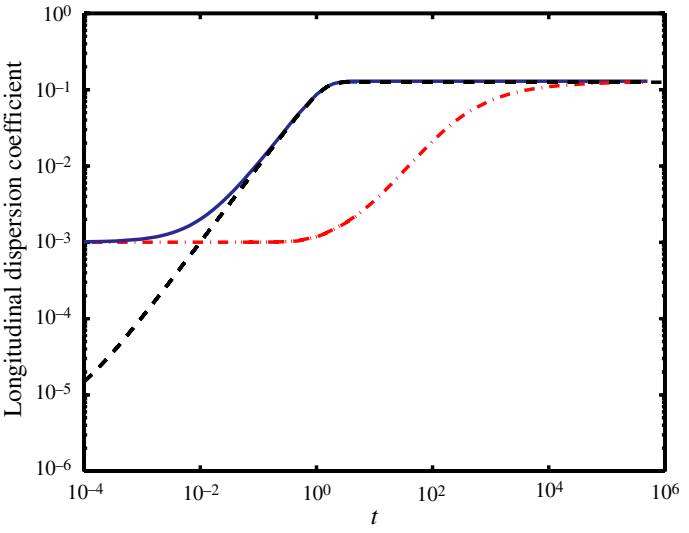

FIGURE 2. (Colour online) Longitudinal dispersion coefficients in two dimensions for Gaussian longitudinal correlation function (in all cases $D_{ii} = D$). Ensemble for $D = 0$ (black, dashed), ensemble for $D = 10^{-3}$ (blue, full) and effective for $D = 10^{-3}$ (red, dotted-dashed). In all cases $\sigma^2 = 0.1$.

constant value of 1:

$$C_1(x_1) = (\beta - 1) \int_0^1 \mathrm{d}k_1 \, k_1^{\beta-2} + \cdots = 1 + \cdots, \tag{3.27}$$

where the dots denote sub-leading contributions of $O(x_1)$. For $x_1 \gg 1$, (3.26) can be approximated by

$$C_1(x_1) = x_1^{1-\beta}(\beta - 1) \int_0^{x_1} \mathrm{d}k_1 \cos(k_1) k_1^{\beta-2} = B(\beta) x_1^{1-\beta} + \cdots. \tag{3.28}$$

This displays a pure power-law behaviour $C_1(x_1) \sim x_1^{1-\beta}$ at large distances. Here, $B(\beta)$ is a constant that depends on β, defined as

$$B(\beta) \equiv (\beta - 1) \int_0^\infty \mathrm{d}k_1 \cos(k_1) k_1^{\beta-2} = \Gamma(\beta) \sin\left(\frac{\beta\pi}{2}\right). \tag{3.29}$$

An illustration of this power-law correlation function (3.27) is depicted in figure 1. The Fourier transform of correlation function (3.26) is given by

$$\widetilde{C}_1(k_1) = (\beta - 1)\pi \, |k_1|^{\beta-2} \, \Theta(1 - |k_1|), \tag{3.30}$$

where $\Theta(x)$ is the Heaviside step function.

Inserting (3.26) into expressions (3.18) and (3.19) for the longitudinal ensemble and effective dispersion coefficients, we obtain the integral expressions

$$D_{11}^{ens}(t) = \sigma^2(\beta - 1) \int_0^t \mathrm{d}t' \prod_{i=2}^{d} (1 + 2D_{ii}t')^{-1/2} \int_0^1 \mathrm{d}k_1 \cos(k_1 t') \, |k_1|^{\beta-2}, \tag{3.31}$$

$$D_{11}^{eff}(t) = D_{11}^{ens}(t) - \sigma^2(\beta - 1)\int_0^t \mathrm{d}t' \prod_{i=2}^{d} (1 - 2D_{ii}t' + 4D_{ii}t)^{-1/2} \times \int_0^1 \mathrm{d}k_1 \cos(k_1 t')\,|k_1|^{\beta-2}\,. \tag{3.32}$$

We distinguish different time regimes that are separated by the (dimensionless) advection time scale $\tau_u = 1$ and the dispersion times scales $\tau_{D_i} = 1/D_{ii}$ for $i = 1, \ldots, d$. In order to simplify the following analysis, we assume that $D_{ii} = D$. Thus, we distinguish three different time regimes that are separated by $\tau_u = 1$ and $\tau_D = 1/D$; recall that $\tau_D \gg \tau_u$.

In the short-time regime $t \ll \tau_u$, the effective dispersion coefficient (3.32) is of the order of D_{11}. The ensemble dispersion coefficient (3.31) shows the ballistic behaviour given by (3.23). For times large compared to the advection time, $t \gg \tau_u$, (3.31) and (3.32) can be approximated by

$$D_{11}^{ens}(t) = \sigma^2 B(\beta)\int_0^t \mathrm{d}t'\, t'^{1-\beta}\,(1 + 2Dt')^{-(d-1)/2} + \cdots, \tag{3.33}$$

$$D_{11}^{eff}(t) = D_{11}^{ens}(t) - \sigma^2 B(\beta)\int_0^t \mathrm{d}t'\, t'^{1-\beta}\,(1 - 2Dt' + 4Dt)^{-(d-1)/2} + \cdots, \tag{3.34}$$

where the dots denote sub-leading contributions and $B(\beta)$ is defined by (3.29).

In the intermediate-time regime $\tau_u \ll t \ll \tau_D$, expressions (3.33) and (3.34) for the ensemble and effective dispersion coefficients can be further approximated as

$$D_{11}^{ens}(t) = \sigma^2 \frac{B(\beta)}{2-\beta} t^{2-\beta} + \cdots, \tag{3.35}$$

$$D_{11}^{eff}(t) = \sigma^2 \frac{B(\beta) 2D(d-1)}{2-\beta} t^{3-\beta} + \cdots. \tag{3.36}$$

In the long-time limit $t \gg \tau_D$, the ensemble and effective dispersion coefficients are equal to leading order,

$$D_{11}^{eff}(t) = D_{11}^{ens}(t) + \cdots. \tag{3.37}$$

In order to extract the leading behaviour in the limit $t \gg \tau_D$, we rescale (3.33) such that

$$D_{11}^{ens}(t) = \sigma^2 B(\beta) D^{\beta-2}\int_0^{t/\tau_D} \mathrm{d}t'\, t'^{1-\beta}\,(1 + 2t')^{-(d-1)/2} + \cdots. \tag{3.38}$$

As can be seen from the behaviour of the integrand for large t', the integral exists in the limit $t/\tau_D \to \infty$ for $\beta > (5-d)/2$. In this case, both ensemble and effective dispersion coefficients converge in the long-time regime $t \gg \tau_D$ to the constant asymptotic value

$$\begin{aligned} D_{11}^{ens}(t) &= \sigma^2 B(\beta) D^{\beta-2}\int_0^{\infty} \mathrm{d}t'\, t'^{1-\beta}\,(1 + 2t')^{-(d-1)/2} + \cdots \\ &= \sigma^2 B(\beta)\frac{(2D)^{\beta-2}\,\Gamma[(d-1)/2 + \beta - 2]\Gamma(2-\beta)}{\Gamma[(d-1)/2]} + \cdots. \end{aligned} \tag{3.39}$$

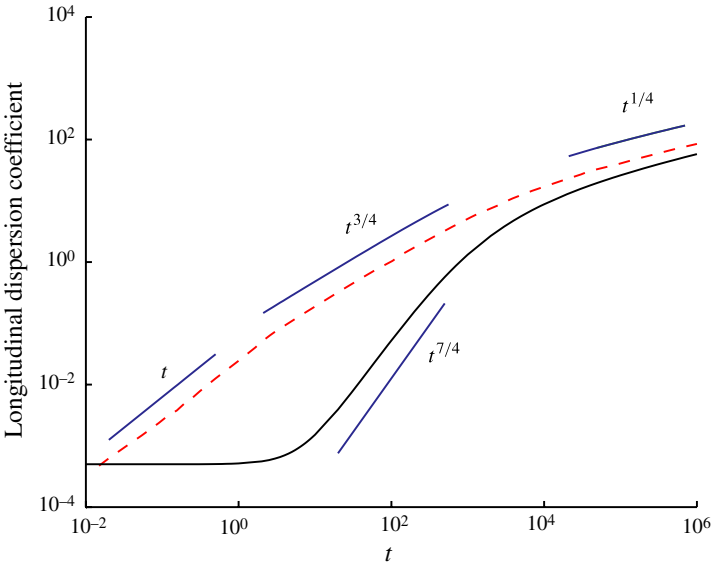

FIGURE 3. (Colour online) Longitudinal dispersion coefficients in two dimensions for the power-law longitudinal correlation function with $\beta = 5/4$ (in all cases $D_{ii} = D$). Ensemble for $D = 5 \times 10^{-4}$ (red, dashed) and effective for $D = 5 \times 10^{-4}$ (black, full). In all cases $\sigma^2 = 0.1$. Note the three distinct power-law regimes that scale as t, $t^{3/4}$ and $t^{1/4}$ for the ensemble dispersion coefficient, and the $t^{7/4}$ regime in the effective dispersion coefficient.

In the case of $\beta < (5 - d)/2$, the integral diverges in the limit $t \gg \tau_D$. By rescaling (3.38) again, we obtain

$$D_{11}^{ens}(t) = \sigma^2 D^{\beta-2} B(\beta) \left(\frac{t}{\tau_D}\right)^{(5-d)/2-\beta} \int_0^1 \mathrm{d}t'\, t'^{1-\beta} \left(\tau_D/t + 2t'\right)^{-(d-1)/2} + \cdots. \quad (3.40)$$

The integral can be evaluated in the limit $t/\tau_D \to \infty$, which gives the following leading-order behaviour for $D_{11}^{ens}(t)$:

$$D_{11}^{ens}(t) = \sigma^2 B(\beta) \frac{D^{\beta-2} 2^{-(d-1)/2}}{(5-d)/2 - \beta} \left(\frac{t}{\tau_D}\right)^{(5-d)/2-\beta} + \cdots. \quad (3.41)$$

The dispersion coefficients converge to a constant asymptotic value for $\beta > (5 - d)/2$ and scale as a power law for $\beta < (5 - d)/2$. For example, for $d = 3$, the dispersion coefficient converges to a constant value for all $\beta > 1$, in $d = 2$ for $\beta \geqslant 3/2$. This highlights how important the dimensionality of the problem at hand is when calculating effective dispersion coefficients (e.g. Attinger, Dentz & Kinzelbach 2004).

The behaviour predicted here is illustrated in figures 3 and 4, for two different power laws, namely $\beta = 7/4$ and $5/4$ for a system where $d = 2$. These two different values, one greater than and one less than $\beta = 3/2$, were chosen to illustrate the late-time difference as predicted by (3.39) and (3.41).

3.1.3. *Truncated power-law correlation*

The final correlation function that we consider is that of a truncated power law. While the power-law correlation function in the previous section provides a lot of insight, the fractal behaviour of such a correlation function is highly unlikely to truly occur at all scales in nature. As such, we consider a similar correlation function that

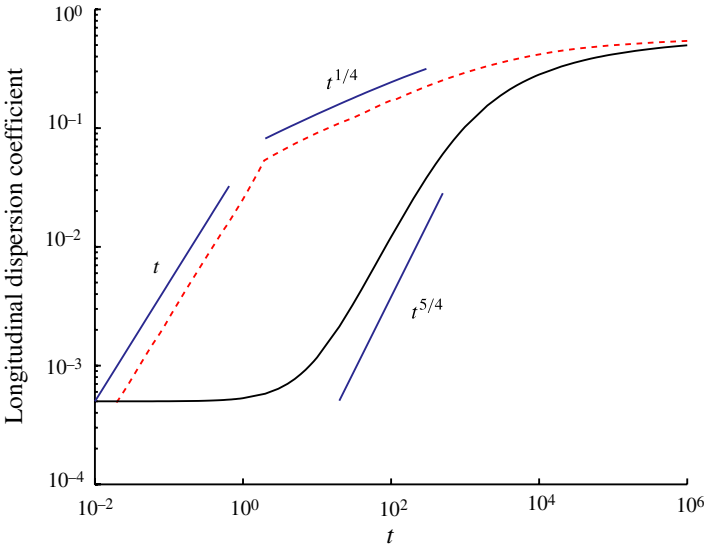

FIGURE 4. (Colour online) Longitudinal dispersion coefficients in two dimensions for the power-law correlation function with $\beta = 7/4$ (in all cases $D_{ii} = D$). Ensemble for $D = 5 \times 10^{-4}$ (red, dashed) and effective for $D = 5 \times 10^{-4}$ (black, full). In all cases $\sigma^2 = 0.1$. Note the two distinct power-law regimes that scale as t and $t^{1/4}$ as well as the late-time asymptote to a constant value for the ensemble dispersion coefficient, and the $t^{5/4}$ scaling for the effective one.

displays the power-law behaviour over large distances, but is cut off at a distance larger than some critical value. A correlation function that displays such behaviour is given by

$$C_1(x_1) = \frac{\exp(-|x_1|/\ell_c)}{(1 + |x_1|)^{\beta-1}}. \tag{3.42}$$

The autocorrelation function (3.42) is illustrated in figure 1 for $\beta = 3/2$ and $\ell_c = 10^5$. As for the power-law correlation function (3.26), the smallest typical heterogeneity scale is of order 1. The dimensionless length scale ℓ_c defines the cutoff scale. For distances large compared to ℓ_c, the correlation decreases exponentially, that is, on an observation scale large compared to ℓ_c the medium again appears homogeneous. For an observation scale L between 1 and ℓ_c, $1 \ll L \ll \ell_c$, the medium appears heterogeneous.

For the transport dynamics in the truncated power-law correlated random field, we distinguish between two dimensionless advection time scales, namely the advection scale $\tau_u = 1$ and the cutoff time scale $\tau_c = \ell_c$.

We obtain the longitudinal ensemble and effective dispersion coefficients by inserting (3.42) into (3.18) and (3.19). This yields

$$D_{11}^{ens}(t) = \sigma^2 \int_0^t \mathrm{d}t' \, \frac{\exp(-t'/\tau_c)}{(1+t')^{\beta-1}} \prod_{i=2}^{d} (1 + 2D_{ii}t')^{-1/2} + \cdots, \tag{3.43}$$

$$D_{11}^{eff}(t) = D_{11}^{ens}(t) - \sigma^2 \int_0^t \mathrm{d}t' \, \frac{\exp(-t'/\tau_c)}{(1+t')^{\beta-1}} \prod_{i=2}^{d} (1 - 2D_{ii}t' + 4D_{ii}t)^{-1/2} + \cdots, \tag{3.44}$$

where the dots denote sub-leading contributions. The cutoff time scale τ_c induces a further time regime. Again, in order to facilitate the analysis, we assume that $D_{ii} = D$, such that we can distinguish four time regimes separated by τ_u, τ_D and τ_c. In the early-time regime $t \ll \tau_u$, the behaviour of the ensemble coefficient is ballistic, given by (3.23), and the effective coefficient is of the order of D_{11}. For the intermediate- and late-time regimes, we consider two different orders of scales: case 1 is defined by $\tau_u \ll \tau_D \ll \tau_c$ and case 2 by $\tau_u \ll \tau_c \ll \tau_D$.

Case 1 ($\tau_u \ll \tau_D \ll \tau_c$). In the intermediate regimes $\tau \ll t \ll \tau_D$ and $\tau_D \ll t \ll \tau_c$, the behaviour of the effective and ensemble dispersion coefficients is the same as in the case of a pure power-law correlation, as discussed in the previous section, because in these regimes the cutoff has no effect. In the long-time regime $t \gg \tau_C$, both ensemble and effective dispersion coefficients converge to the same constant value, which is given by

$$D_{11}^{ens}(t) = \sigma^2 \tau_c^{2-\beta} \exp(1/\tau_c) \Gamma(2-\beta, 1/\tau_c) + \cdots, \tag{3.45}$$

where the dots denote sub-leading contributions. Note that this asymptotic value depends on the cutoff scale τ_c and on the exponent β. Unlike the pure power-law case, the anomalous scaling of dispersion coefficient in time does not occur at long times due to the presence of the cutoff length in the correlation function.

Case 2 ($\tau_u \ll \tau_c \ll \tau_D$). In the intermediate regime $\tau_u \ll t \ll \tau_c$, the effective dispersion coefficient is still of the order of D_{11} because the solute has not yet sampled a sufficient part of the medium heterogeneity by transverse dispersion. The ensemble dispersion coefficient in this regime behaves in leading order as

$$D_{11}^{ens}(t) = \frac{\sigma^2}{(2-\beta)} t^{2-\beta} + \cdots, \tag{3.46}$$

where the dots denote sub-leading contributions. In the time regime defined by $\tau_c \ll t \ll \tau_D$, the ensemble dispersion coefficient converges towards the constant value given by (3.45). The effective dispersion coefficient can be approximated by

$$D_{11}^{eff}(t) = \sigma^2 \tau_c^{2-\beta} \exp(1/\tau_c) \Gamma(2-\beta, 1/\tau_c) \left[1 - \left(1 + \frac{4t}{\tau_D} \right)^{-(d-1)/2} \right] + \cdots. \tag{3.47}$$

In the asymptotic time regime $t \gg \tau_D$, the effective and ensemble coefficients converge to the same constant value (3.45).

The behaviour of the effective and ensemble dispersion coefficients as given by (3.43) and (3.44) are illustrated in figure 5 for $d = 2$, $\beta = 5/4$ and $\ell_c = 10^5$.

4. Random walk particle tracking simulations

In order to test the theoretical expressions derived in this work, we perform a series of numerical simulations. Many approaches for the description of the transport of a solute use the equivalent transport formulation in the Lagrangian framework (Kinzelbach 1987; Andricevic & Cvetkovic 1998; Dentz *et al.* 2003). To do so, we transform the transport problem from the Fokker–Planck framework to the equivalent Lagrangian framework. In order to make this transformation, we have to consider the transport equation for the total concentration distribution, which in non-dimensional terms is

$$c(\boldsymbol{x}, t) = [1 + r(\boldsymbol{x})] g(\boldsymbol{x}, t). \tag{4.1}$$

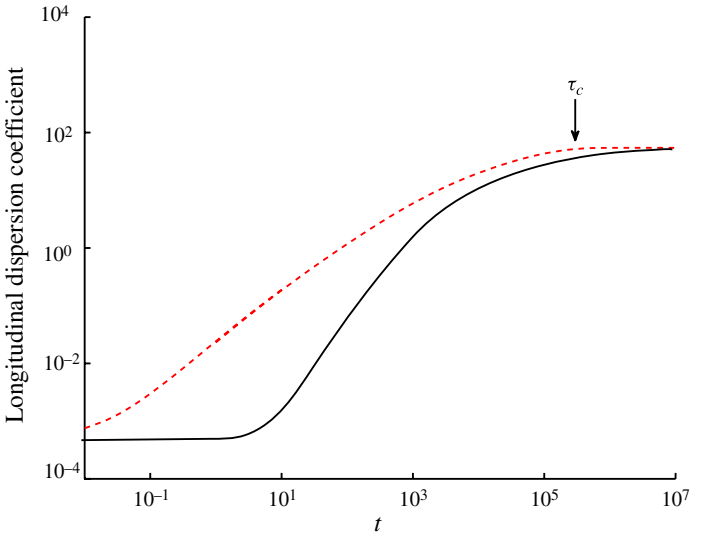

FIGURE 5. (Colour online) Longitudinal dispersion coefficients in two dimensions for the truncated power-law correlation function with $\beta = 5/4$ and $\tau_c = 2 \times 10^5$ (in all cases $D_{ii} = D$). Ensemble (red, dashed) and effective (black, full) dispersion coefficients for $D = 5 \times 10^{-4}$. In all cases $\sigma^2 = 0.1$. Note the early- and intermediate-time power-law-type regime that is cut off at times larger than τ_c leading to a constant asymptotic value.

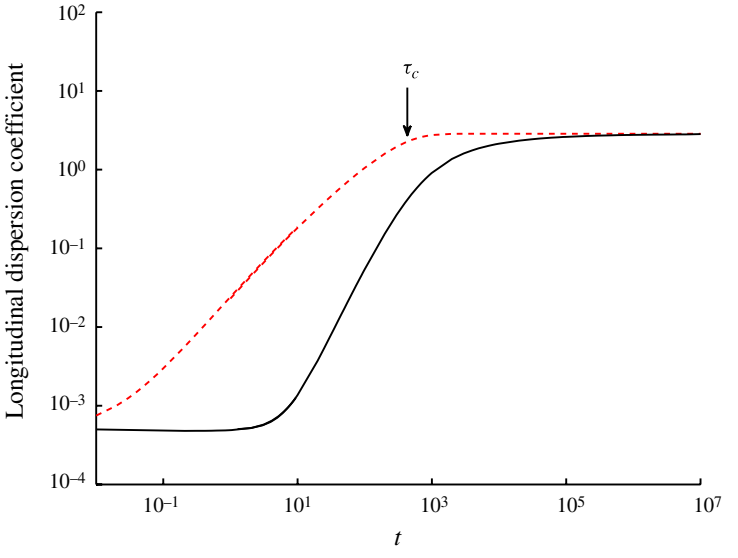

FIGURE 6. (Colour online) Longitudinal dispersion coefficients in two dimensions for the truncated power-law correlation function with $\beta = 5/4$ and $\tau_c = 4 \times 10^2$ (in all cases $D_{ii} = D$). Ensemble (red, dashed) and effective (black, full) dispersion coefficients for $D = 5 \times 10^{-4}$. In all cases $\sigma^2 = 0.1$. Note the early-time power-law-type regime that is cut off at times close to τ_c leading to a constant asymptotic value.

The Fokker–Planck equation for $c(\boldsymbol{x}, t)$ is obtained by using (4.1) in (2.14),

$$\frac{\partial c(\boldsymbol{x}, t)}{\partial t} + \frac{\partial}{\partial x_1} \frac{1}{1 + r(\boldsymbol{x})} c(\boldsymbol{x}, t) - \boldsymbol{\nabla} \otimes \boldsymbol{\nabla} \frac{\boldsymbol{D}}{1 + r(\boldsymbol{x})} c(\boldsymbol{x}, t) = 0, \tag{4.2}$$

where $\otimes$ denotes the tensor product. This Fokker–Planck equation is equivalent to the Langevin equation (see e.g. Risken 1992)

$$\frac{\mathrm{d}x_i(t)}{\mathrm{d}t} = \frac{\delta_{i1}}{1 + r[\boldsymbol{x}(t)]} + \sqrt{\frac{2D_{ii}}{1 + r[\boldsymbol{x}(t)]}} \xi_i(t), \tag{4.3}$$

where the Ito interpretation is used (e.g. Risken 1992). Here, $\boldsymbol{\xi}(t)$ is a white Gaussian noise with zero mean and correlation given by

$$\langle \xi_i(t) \xi_j(t') \rangle = \delta_{ij} \delta(t - t'), \tag{4.4}$$

where the angular brackets denote the average over white noise realizations. The concentration $c(\boldsymbol{x}, t)$, in terms of the particle trajectories $\boldsymbol{x}(t)$, is given by

$$c(\boldsymbol{x}, t) = \langle \delta[\boldsymbol{x} - \boldsymbol{x}(t)] \rangle. \tag{4.5}$$

The initial condition $c(\boldsymbol{x}, t) = \delta(\boldsymbol{x})$ implies that $\boldsymbol{x}(t = 0) = \boldsymbol{0}$.

4.1. *Numerical implementation*

The numerical solution of the transport problem is implemented using random walk simulations that are based on Langevin equation (4.3). In discrete time, the equation governing the position of a solute particle n, $\boldsymbol{x}^{(n)}(t)$, is given by

$$x_i^{(n)}(t + \Delta t) = x_i^{(n)}(t) + \frac{\delta_{i1} \Delta t}{1 + r[\boldsymbol{x}^{(n)}(t)]} + \sqrt{\frac{2D_{ii} \Delta t}{1 + r[\boldsymbol{x}^{(n)}(t)]}} \eta_i^{(n)}(t), \tag{4.6}$$

where the η_i are independent Gaussian random variables with zero mean and unit variance. In the numerical simulations, for simplicity, we set $D_{ii} = D$. Within a given realization, the longitudinal moments of the plume can be calculated from the particle positions, with the ith moment in realization j defined as

$$\mu_j^{(i)}(t) = \lim_{N \to \infty} \frac{1}{N} \sum_{n=1}^{N} [x_1^{(n,j)}(t)]^i, \quad j = 1, \ldots, M, \tag{4.7}$$

where M is the number of realizations of $r(\boldsymbol{x})$, and $x_1^{(n,j)}(t)$ is the trajectory of particle n in realization j. The ensemble and effective dispersion coefficients are defined as

$$D_{11}^{ens}(t) = \frac{1}{2} \frac{\mathrm{d}}{\mathrm{d}t} \lim_{M \to \infty} \frac{1}{M} \left[\sum_{j=1}^{M} \mu_j^{(2)}(t) - \sum_{j=1}^{M} \mu_j^{(1)}(t) \sum_{j=1}^{M} \mu_j^{(1)}(t) \right], \tag{4.8}$$

$$D_{11}^{eff}(t) = \frac{1}{2} \frac{\mathrm{d}}{\mathrm{d}t} \lim_{M \to \infty} \frac{1}{M} \left[\sum_{j=1}^{M} \mu_j^{(2)}(t) - \sum_{j=1}^{M} \mu_j^{(1)}(t) \times \mu_j^{(1)}(t) \right]. \tag{4.9}$$

4.2. *Results*

Comparison between the results of numerical simulations and our theoretical predictions is shown for six cases in figure 7. Simulations were conducted for one system with a Gaussian correlation and for two systems with power-law correlations ($\beta = 5/4$ and $\beta = 7/4$). For each system, the case of vanishing local

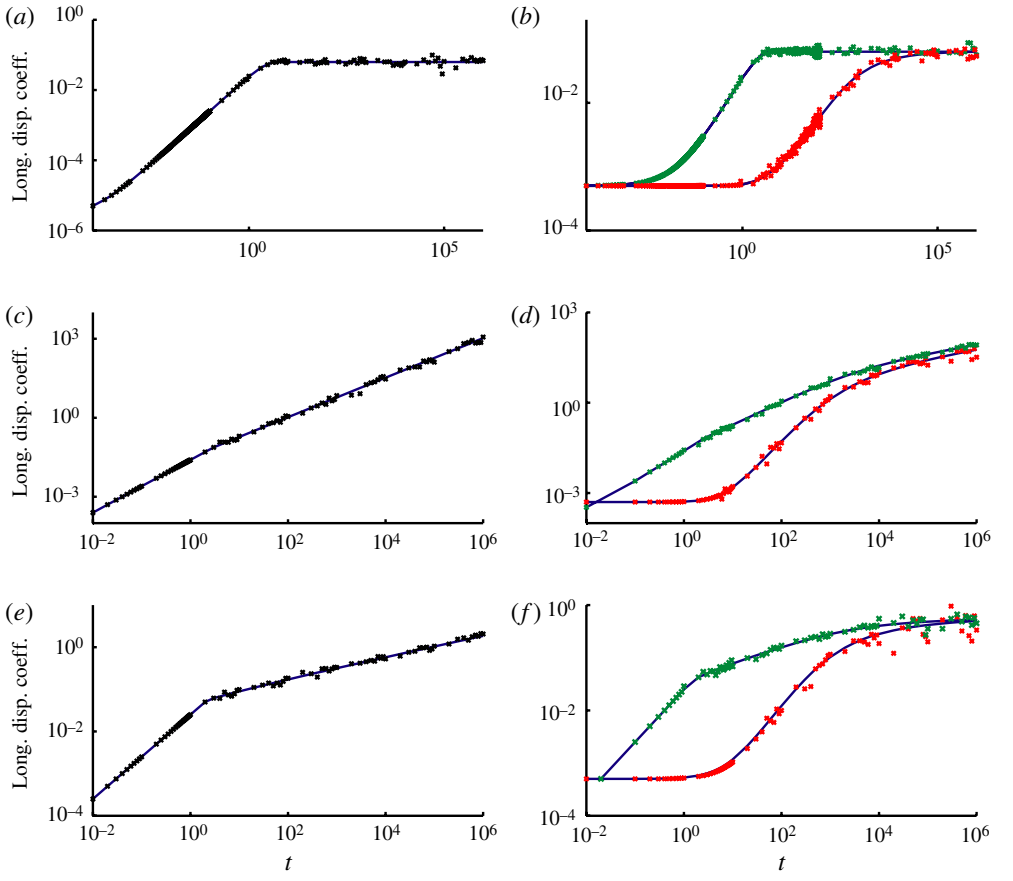

FIGURE 7. (Colour online) Comparison of numerical simulations and analytical predictions. In all cases $\sigma^2 = 0.1$. Ensemble and effective dispersion coefficients are shown. Solid lines correspond to the theoretical predictions, while the symbols correspond to estimates from the numerical simulations. (*a*,*b*) Gaussian longitudinal correlation function; (*c*,*d*) pure power-law correlation with $\beta = 5/4$ and (*e*,*f*) pure power-law correlation with $\beta = 7/4$. In all cases the agreement is good. (*a*,*c*,*e*) $D = 0$ and (*b*,*d*,*f*) $D = 5 \times 10^{-4}$.

dispersion ($D = 0$) and finite, but small, dispersion ($D = 10^{-3}$) were considered. The variances associated with the heterogeneous field are set to $\sigma^2 = 0.1$. Between 10^3 and 10^6 realizations were run for each case. In all cases the predicted behaviour was clearly visible after 10^3 realizations, but more were run to smooth noise.

In all six cases the agreement between theory and simulations is very good, demonstrating all the quantitative and qualitative aspects associated with each of the cases discussed earlier in the text (e.g. the three power-law regimes associated with the power-law correlation and $\beta < 3/2$). In particular, it is clear that the power-law correlation can result in long-time anomalous transport even for weakly heterogeneous random fields.

5. Effective transport equation

When dealing with a heterogeneous system, it is ultimately desirable to obtain an upscaled effective equation that describes the mean transport without requiring the

details of the heterogeneity structure. In this section, we derive an effective equation for the ensemble-averaged mobile concentration.

5.1. *Laplace space formulations of transport*

For technical convenience, we perform a Laplace transform (e.g. Abramowitz & Stegun 1965) of integral equation (2.21) for the Fourier-transformed mobile concentration $\widetilde{g}(\boldsymbol{k}, t)$. The asterisk denotes Laplace-transformed quantities (i.e. $\mathscr{L}\{f(t)\} = f^*(s)$). In Fourier–Laplace space the ensemble-averaged $\widetilde{g}^*(\boldsymbol{k}, s)$ is

$$\overline{\widetilde{g}^*}(\boldsymbol{k}, s) = \widetilde{g}_0^*(\boldsymbol{k}, s) - \widetilde{g}_0^*(\boldsymbol{k}, s) \int_{k'} s\overline{\widetilde{r}(\boldsymbol{k}')\widetilde{g}^*(\boldsymbol{k} - \boldsymbol{k}', s)}. \tag{5.1}$$

From this expression, we can implicitly define the self-energy $\Sigma(\boldsymbol{k}, s)$ as

$$\overline{\widetilde{g}^*}(\boldsymbol{k}, s) = \{s[1 - \Sigma(\boldsymbol{k}, s)] - \mathrm{i}k_1 + \boldsymbol{k} \cdot \boldsymbol{D} \cdot \boldsymbol{k}\}^{-1}. \tag{5.2}$$

For moderate heterogeneity, by perturbation theory,

$$\Sigma(\boldsymbol{k}, s) \equiv s\sigma^2 \int_{k'} \widetilde{C}_{\mu\mu}(\boldsymbol{k}')\widetilde{g}_0^*(\boldsymbol{k} - \boldsymbol{k}', s). \tag{5.3}$$

From (5.2) we obtain an effective equation for the ensemble-averaged mobile concentration:

$$s[1 - \Sigma(\boldsymbol{k}, s)]\overline{\widetilde{g}^*}(\boldsymbol{k}, s) = 1 + (\mathrm{i}k_1 - \boldsymbol{k} \cdot \boldsymbol{D} \cdot \boldsymbol{k})\overline{\widetilde{g}^*}(\boldsymbol{k}, s). \tag{5.4}$$

From this equation, we identify the total average concentration as

$$\overline{\widetilde{c}^*}(\boldsymbol{k}, s) = [1 - \Sigma(\boldsymbol{k}, s)]\overline{\widetilde{g}^*}(\boldsymbol{k}, s). \tag{5.5}$$

The corresponding effective transport equation for the total average concentration then reads:

$$s\overline{\widetilde{c}^*}(\boldsymbol{k}, s) - \frac{\mathrm{i}k_1}{[1 - \Sigma(\boldsymbol{k}, s)]}\overline{\widetilde{c}^*}(\boldsymbol{k}, s) + \frac{\boldsymbol{k} \cdot \boldsymbol{D} \cdot \boldsymbol{k}}{[1 - \Sigma(\boldsymbol{k}, s)]}\overline{\widetilde{c}^*}(\boldsymbol{k}, s) = 1. \tag{5.6}$$

5.2. *Generalized master equation and continuous-time random walks*

The CTRW method (e.g. Berkowitz *et al.* 2006) provides an approach for the modelling of anomalous transport in porous media. Here we seek a formulation of the transport problem in terms of a CTRW. To this end we rewrite (5.4) for the average non-adsorbed concentration $\overline{\widetilde{g}^*}(\boldsymbol{k}, s)$ tautologically as

$$\begin{aligned} &s\{1 - \Sigma(\boldsymbol{0}, s)\}\overline{\widetilde{g}^*}(\boldsymbol{k}, s) \\ &\quad = 1 - s\Sigma(\boldsymbol{0}, s)\overline{\widetilde{g}^*}(\boldsymbol{k}, s) + (\mathrm{i}k_1 - \boldsymbol{k} \cdot \boldsymbol{D} \cdot \boldsymbol{k} + s\Sigma(\boldsymbol{k}, s))\overline{\widetilde{g}^*}(\boldsymbol{k}, s). \end{aligned} \tag{5.7}$$

Let us define the concentration $\overline{\widetilde{c}_0^*}(\boldsymbol{k}, s)$ such that

$$\overline{\widetilde{c}_0^*}(\boldsymbol{k}, s) = [1 - \Sigma(\boldsymbol{0}, s)]\overline{\widetilde{g}^*}(\boldsymbol{k}, s), \tag{5.8}$$

which is related to the average total concentration by

$$\overline{\widetilde{c}_0^*}(\boldsymbol{k}, s) = \frac{1 - \Sigma(\boldsymbol{0}, s)}{1 - \Sigma(\boldsymbol{k}, s)}\overline{\widetilde{c}^*}(\boldsymbol{k}, s). \tag{5.9}$$

Using (5.8) in (5.7), we obtain the following equation for $\overline{\widetilde{c}_0^*}(\boldsymbol{k}, s)$:

$$s\overline{\widetilde{c}_0^*}(\boldsymbol{k}, s) = 1 + \widetilde{\phi}^*(\boldsymbol{k}, s)\overline{\widetilde{c}_0^*}(\boldsymbol{k}, s) - \widetilde{\phi}^*(\boldsymbol{0}, s)\overline{\widetilde{c}_0^*}(\boldsymbol{k}, s), \tag{5.10}$$

where

$$\widetilde{\phi}^*(\boldsymbol{k}, s) \equiv \frac{1 + \mathrm{i}k_1 - \boldsymbol{k} \cdot \boldsymbol{D} \cdot \boldsymbol{k}}{1 - \Sigma(\boldsymbol{0}, s)} + \frac{s\Sigma(\boldsymbol{k}, s)}{1 - \Sigma(\boldsymbol{0}, s)}. \tag{5.11}$$

Equation (5.10) is the Fourier–Laplace transform of a generalized master equation (e.g. Kenkre, Montroll & Schlesinger 1973), which in real time and space can be written as

$$\frac{\partial}{\partial t}\overline{c}_0(\boldsymbol{x}, t) = \int_0^t \mathrm{d}t' \int \mathrm{d}^d x' \, \phi(\boldsymbol{x} - \boldsymbol{x}', t - t')\{\overline{c}_0(\boldsymbol{x}', t') - \overline{c}_0(\boldsymbol{x}, t')\}. \tag{5.12}$$

In the framework of CTRW, an effective transport equation is given by (e.g. Dentz & Berkowitz 2003; Berkowitz *et al.* 2005):

$$s\overline{\widetilde{c}_0^*}(\boldsymbol{k}, s) = 1 + \frac{s\widetilde{\psi}^*(\boldsymbol{k}, s)}{1 - \psi^*(s)}\overline{\widetilde{c}_0^*}(\boldsymbol{k}, s) - \frac{s\psi^*(s)}{1 - \psi^*(s)}\overline{\widetilde{c}_0^*}(\boldsymbol{k}, s), \tag{5.13}$$

where $\widetilde{\psi}^*(\boldsymbol{k}, s)$ denotes the joint transition length and time distribution, and $\psi^*(s) \equiv \widetilde{\psi}^*(\boldsymbol{0}, s)$. Comparing (5.10) with definition (5.11) and (5.13), we obtain the following relation between the joint transition length and time distribution $\widetilde{\psi}^*(\boldsymbol{k}, s)$ and $\Sigma(\boldsymbol{k}, s)$:

$$\widetilde{\psi}^*(\boldsymbol{k}, s) = \frac{1 + \mathrm{i}k_1 - \boldsymbol{k} \cdot \boldsymbol{D} \cdot \boldsymbol{k}}{1 + s} + \frac{s\Sigma(\boldsymbol{k}, s)}{1 + s}. \tag{5.14}$$

The first term on the right-hand side gives the local transport behaviour in a homogeneous medium. The second term represents the disorder-induced contribution. Note that, in this heterogeneity-induced contribution, the space and time dependences are intrinsically coupled, i.e. $\widetilde{\psi}^*(\boldsymbol{k}, s)$ cannot in general be decoupled into a part that depends on time and one that depends on space only.

In order to illustrate the structure of the distribution, we will focus on $\psi(t)$, whose Laplace transform is

$$\psi^*(s) = \frac{1}{1 + s} + \frac{s\Sigma(0, s)}{1 + s}. \tag{5.15}$$

The function $\psi(t)$ is illustrated in figure 8 for three cases. The first corresponds to transport in a homogeneous medium (i.e. only the first term on the right-hand side of (5.15)); the second corresponds to a chemically heterogeneous medium with Gaussian correlation; and the third corresponds to a chemically heterogeneous medium with power-law correlation. For the homogeneous case, $\psi(t)$ is an exponential distribution with a very rapid cutoff at high values of t. The case with Gaussian correlation looks quite similar, with an exponential cutoff at large values of t. This is a reflection of the fact that this system in the long run returns to behaving in a Fickian manner. The main difference between the homogeneous and Gaussian correlated cases is that the system with the Gaussian correlation has a greater weight at larger values of t, reflecting the influence of heterogeneity and enhanced dispersion. Finally, $\psi(t)$ associated with the power-law correlation structure also displays a power-law tail at high values of t, reflecting the enhanced and sustained anomalous dispersion at long times.

6. Conclusion

In this work we study the influence that correlation structure plays on transport in fields with heterogeneous retardation coefficient. In order to isolate the influence of correlation, we restricted our study to fields with relatively weak degrees of

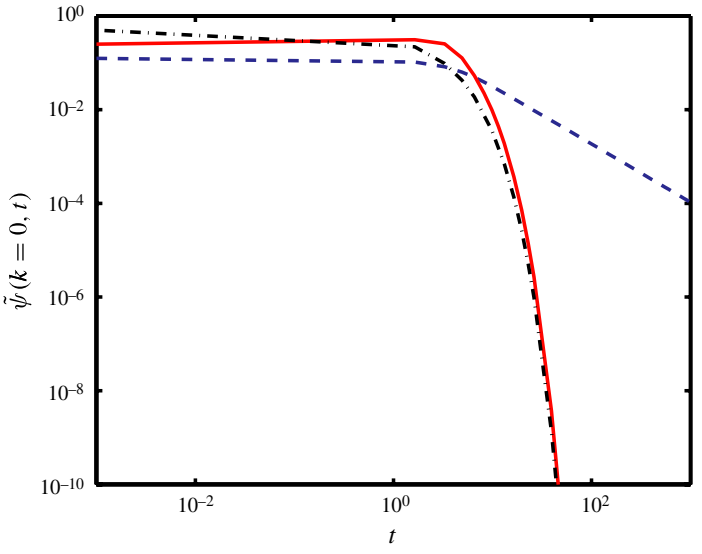

FIGURE 8. (Colour online) The function $\widetilde{\psi}(0,t)$ for the homogeneous case (black,dotted-dashed), the heterogeneous system with Gaussian correlation (red, full) and the heterogeneous system with a power-law correlation with $\beta = 5/4$ (blue, dashed). For all cases $D = 0$.

heterogeneity, which in turn allowed us to reliably use a perturbation method approach. The objective of the paper was to study how correlation in the retardation field impacts large-scale transport.

The large-scale transport behaviour was investigated in terms of the ensemble and effective dispersion coefficients, which are measures for the extent of the concentration distribution. To highlight and isolate the influence that correlation plays, we focused on correlation functions that display short-range (Gaussian), intermediate-range (truncated power law) and long-range (power law) correlation.

For the short-range correlation structures, we recover expressions similar to previously derived ones. After an initial transient, the late-time dispersion coefficients converge to a constant value. On the other hand, the long-range power-law correlation structures display anomalous scalings in the effective and ensemble dispersion coefficients, whose persistence depends on the dimensionality of space as well as the exponent associated with the power-law correlation function. We identify several time regimes of anomalous dispersion characterized by different scaling exponents. Interestingly, the evolution of the ensemble dispersion coefficient, which for short-range correlation is determined solely by the advection time scale, is for strong disorder correlation and at large times governed by the dispersion time scale. For intermediate range correlation, a rich behaviour can be observed that displays several regimes of preasymptotic anomalous dispersion. The analytical results were complemented by a series of numerical random walk particle tracking simulations, which are in good agreement with the derived behaviour.

To conclude this paper, we developed an effective large-scale equation for transport under random retardation and in particular demonstrate that it falls into the broad category of CTRW models. The coupled transition length and time distribution $\psi(\boldsymbol{x}, t)$, which lies at the heart of the CTRW transport model, consists of a part characterizing transport in a homogeneous medium and a disorder-induced part that

was determined using perturbation theory. While the homogeneous part is decoupled, the heterogeneous part is in general characterized by a coupling of the transition length and time. The derived behaviour of the ensemble and effective dispersion coefficients shed some new light on the local-scale transport and disorder mechanisms that can lead to large-scale anomalous dispersion behaviour and its quantification in terms of an effective transport equation.

While the model presented here is highly idealized, it highlights that anomalous transport can occur in weakly heterogeneous media due to correlation structure. Thus one should be cautious in inferring the cause of anomalous transport from dispersion data alone. However, should local knowledge of typical ranges of chemical heterogeneity values be known, observations of anomalous transport could be used to infer correlation structure of the heterogeneity within the medium. Additionally, the derivation of the effective CTRW model demonstrates how CTRW model parameters may be linked to the underlying heterogeneity structure.

Acknowledgements

D.B. would like to express thanks for financial support via NSF grant EAR-1113704. M.D. acknowledges the financial support of the Spanish Ministry of Science and Innovation (MICINN) through the project HEART (CGL2010-18450). Any opinions, findings, conclusions or recommendations do not necessarily reflect the views of the funding agencies.

REFERENCES

ABRAMOWITZ, M. & STEGUN, I. A. 1965 *Handbook of Mathematical Functions: with Formulas, Graphs, and Mathematical Tables*. Dover.

ADAMS, E. E. & GELHAR, L. W. 1992 Field study of dispersion in a heterogeneous aquifer, 2, spatial moments analysis. *Water Resour. Res.* **28** (12), 3293–3307.

ANDRICEVIC, R. & CVETKOVIC, V. 1998 Relative dispersion for solute flux in aquifers. *J. Fluid Mech.* **361**, 145–174.

ARIS, R. 1956 On the dispersion of a solute in a fluid flowing through a tube. *Proc. R. Soc. Lond.* A **235**, 67.

ATTINGER, S., DENTZ, M. & KINZELBACH, W. 2004 Exact transverse macro dispersion coefficients for transport in heterogeneous porous media. *Stoch. Environ. Res. Risk Assess.* **18**, 9–15.

ATTINGER, S., DENTZ, M., KINZELBACH, H. & KINZELBACH, W. 1999 Temporal behaviour of a solute cloud in a chemically heterogeneous porous medium. *J. Fluid Mech.* **386**, 77–104.

DE BARROS, F. J. & RUBIN, Y. 2011 Modelling of block-scale macrodispersion as a random function. *J. Fluid Mech.* **676**, 514–545.

BATCHELOR, G. K. 1949 Diffusion in a field of homogeneous turbulence I, Eulerian analysis. *Austral. J. Sci. Res.* **2**, 437–450.

BELLIN, A., RINALDO, A., BOSMA, W. J. P., VAN DER ZEE, S. E. A. T. M. & RUBIN, Y. 1993 Linear equilibrium adsorbing solute transport in physically and chemically heterogeneous porous formations: 1. Analytical solutions. *Water Resour. Res.* **29**, 4019–4030.

BELLIN, A., SALANDIN, P. & RINALDO, A. 1992 Simulation of dispersion in heterogeneous porous formations: statistics, first-order theories, convergence of computations. *Water Resour. Res.* **28**, 2211–2227.

BENSON, D. A., WHEATCRAFT, S. W. & MEERSCHAERT, M. M. 2000 Application of a fractional advection–dispersion equation. *Water Resour. Res.* **36**, 1403–1412.

BERKOWITZ, B., CORTIS, A., DENTZ, M. & SCHER, H. 2006 Modeling non-Fickian transport in geological formations as a continuous time random walk. *Rev. Geophys.* **44**, RG2003.

BERKOWITZ, B., KOSAKOWSKI, G., MARGOLIN, G. & SCHER, H. 2005 Application of continuous time random walk theory to tracer test measurements in fractured and heterogeneous porous media. *Ground Water* **39**, 593–604.

BOLSTER, D., DENTZ, M. & LEBORGNE, T. 2009 Solute dispersion in channels with periodically varying apertures. *Phys. Fluids* **21**, 056601.

BOUCHAUD, J.-P. & GEORGES, A. 1990 Anomalous diffusion in disordered media: statistical mechanisms, models and physical applications. *Phys. Rep.* **195**, 127–293.

BRENNER, H. 1980 Dispersion resulting from flow through spatially periodic porous media. *Phil. Trans. R. Soc. Lond. Ser.* A **297**, 81–133.

CHRYSIKOPOULOS, C. V., KITANIDIS, P. K. & ROBERTS, P. V. 1990 Analysis of one-dimensional solute transport through porous media with spatially variable retardation factor. *Water Resour. Res.* **26**, 437–446.

CVETKOVIC, V., DAGAN, G. & CHENG, H. 1998 Contaminant transport in aquifers with spatially variable hydraulic and sorption properties. *Proc. R. Soc. Lond.* A **454**, 2173–2207.

DAGAN, G. 1984 Solute transport in hetereogeneous porous formations. *J. Fluid Mech.* **145**, 151–177.

DAGAN, G. 1990 Transport in heterogeneous porous formations: spatial moments, ergodicity, and effective dispersion. *Water Resour. Res.* **26**, 1281–1290.

DAGAN, G. 1991 Dispersion of a passive solute in non-ergodic transport by steady velocity fields in heterogeneous formations. *J. Fluid Mech.* **233**, 197–210.

DAGAN, G. 1994 The significance of heterogeneity of evolving scales and of anomalous diffusion to transport in porous formations. *Water Resour. Res.* **30**, 3327–3336.

DAGAN, G. & NEUMAN, S. P. (Eds) 1997 *Subsurface Flow and Transport*. Cambridge University Press.

DENTZ, M. & BERKOWITZ, B. 2003 Transport behavior of a passive solute in continuous time random walks and multirate mass transfer. *Water Resour. Res.* **39**, 1111.

DENTZ, M. & BOLSTER, D. 2010 Distribution- versus correlation-induced anomalous transport in quenched random velocity fields. *Phys. Rev. Lett.* **105**, 244301.

DENTZ, M., BOLSTER, D. & LEBORGNE, T. 2009 Concentration statistics for transport in random media. *Phys. Rev.* E **80**, 010101.

DENTZ, M. & CASTRO, A. 2009 Effective transport dynamics in porous media with heterogeneous retardation properties. *Geophys. Res. Lett.* **35**, L03403.

DENTZ, M., KINZELBACH, H., ATTINGER, S. & KINZELBACH, W. 2000 Temporal behaviour of a solute cloud in a heterogeneous porous medium, 1, point-like injection. *Water Resour. Res.* **36** (12), 3591–3604.

DENTZ, M., KINZELBACK, H., ATTINGER, S. & KINZELBACH, W. 2003 Numerical studies of the transport behaviour of a passive solute in a two-dimensional incompressible random flow field. *Phys. Rev.* E **67**, 046306.

DI FEDERICO, V. & ZHANG, Y. K. 1999 Solute transport in heterogeneous porous media with long-range correlations. *Water Resour. Res.* **35**, 3185–3191.

EDWARDS, D. & BRENNER, H. 1993 *Macrotransport Processes*. Butterworth Heinemann.

FIORI, A. 2001 On the influence of local dispersion in solute transport through formations with evolving scales of heterogeneity. *Water Resour. Res.* **37**, 235–242.

GELHAR, L. W. 1992 *Stochastic Subsurface Hydrology*. Prentice-Hall.

GELHAR, L., WELTY, C. & REHFELDT, K. A. 1992 A critical review of data on field scale dispersion in aquifers. *Water Resour. Res.* **28**, 1955–1974.

GILL, W. N. & SANKARASUBRAMANIAN, R. 1970 Exact analysis of unsteady convective diffusion. *Proc. R. Soc. Lond.* A **316**, 341.

GLIMM, J. & SHARP, D. H. 1991 A random field model for anomalous diffusion in heterogeneous porous media. *J. Stat. Phys.* **62**, 415–424.

GRATHWOHL, P. 1998 *Diffusion in Natural Porous Media: Contaminant Transport, Sorption/Desorption and Dissolution Kinetics*. Springer.

HERRICK, M. G., BENSON, D. A., MEERSCHAERT, M. M. & MCCALL, K. R. 2002 Hydraulic conductivity, velocity, and the order of the fractional dispersion derivative in a highly heterogeneous system. *Water Resour. Res.* **38** (11), 1227.

JARMAN, K. D. & TARTAKOVSKY, A. M. 2008 Divergence of solutions to solute transport moment equations. *Geophys. Res. Lett.* **35**, L15401.

JONES, S. W. & YOUNG, W. R. 1994 Shear dispersion and anomalous diffusion by chaotic advection. *J. Fluid Mech.* **280**, 149–172.

KENKRE, V. M., MONTROLL, E. W. & SCHLESINGER, F. M. 1973 Generalized master equations for continuous time random walks. *J. Stat. Phys.* **9**, 45.

KINZELBACH, W. 1987 Methods for the simulation of pollutant transport in ground water: a model comparison. In *Proceedings of the NWWA Conference on Solving Ground Water Problems with Models*, pp. 656–675. National Water Well Association.

KITANIDIS, P. K. 1988 Prediction by the method of moments of transport in heterogeneous formations. *J. Hydrol.* **102**, 453–473.

KOCH, D. L. & BRADY, J. F. 1985 Dispersion in fixed beds. *J. Fluid Mech.* **154**, 399–427.

KOCH, D. L. & BRADY, J. F. 1987 A non-local description of advection–diffusion with application to dispersion in porous media. *J. Fluid Mech.* **180**, 387–403.

LATINI, M. & BERNOFF, A. J. 2001 Transient anomalous diffusion in Poiseuille flow. *J. Fluid Mech.* **441**, 399–411.

LAWRENCE, A. E. & RUBIN, Y. 2007 Block-effective macrodispersion for numerical simulations of sorbing solute transport in heterogeneous porous formations. *Adv. Water Resour.* **30**, 1272–1285.

LEBORGNE, T., DENTZ, M. & CARRERA, J. 2008 Lagrangian statistical model for transport in highly heterogeneous velocity fields. *Phys. Rev. Lett.* **101**, 090601.

LENZ, R. D. & KUMAR, S. 2007 Competitive displacement of thin liquid films on chemically patterned substrates. *J. Fluid Mech.* **571**, 33–57.

LEVY, M. & BERKOWITZ, B. 2003 Measurement and analysis of non-Fickian dispersion in heterogeneous porous media. *J. Contam. Hydrol.* **64**, 203–226.

LUNATI, I., ATTINGER, S. & KINZELBACH, W. 2002 Macrodispersivity for transport in arbitrary nonuniform flow fields: asymptotic and preasymptotic results. *Water Resour. Res.* **38** (10), 1187.

MATHERON, G. & DE MARSILY, G. 1980 Is transport in porous media always diffusive? A counter example. *Water Resour. Res.* **16**, 901.

MIRALLES-WILHELM, F. & GELHAR, L. W. 1996 Stochastic analysis of sorption macrokinetics in heterogeneous aquifers. *Water Resour. Res.* **32**, 1541–1549.

MORONI, M. & CUSHMAN, J. H. 2001 Statistical mechanics with three-dimensional particle tracking velocimetry experiments in the study of anomalous dispersion. I. Theory. *Phys. Fluids* **13**, 75.

NEUMAN, S. P. 1990 Universal scaling of hydraulic conductivities and dispersivities in geologic media. *Water Resour. Res.* **26**, 1749–1758.

NEUMAN, S. P. & TARTAKOVSKY, D. M. 2009 Perspective on theories of anomalous transport in heterogeneous media. *Adv. Water Res.* **32**, 670–680.

RAJARAM, H. & GELHAR, L. W. 1995 Plume-scale dependent dispersion in aquifers with a wide range of scales of heterogeneity. *Water Resour. Res.* **31** (10), 2469–2482.

RISKEN, H. 1992 *The Fokker–Planck Equation*. Springer.

RUBIN, Y., SUN, A., MAXWELL, R. & BELLIN, A. 1999 The concept of block-effective macrodispersivity and a unified approach for grid-scale- and plume-scale-dependent transport. *J. Fluid Mech.* **395**, 161–180.

SANCHEZ-VILA, X. & BOLSTER, D. 2009 An analytical approach to transient homovalent cation exchange problems. *J. Hydrol.* **378**, 281–289.

SILLIMAN, S. E. & SIMPSON, E. S. 1987 Laboratory evidence of the scale effect in dispersion of solutes in porous media. *Water Resour. Res.* **23** (8), 1667–1673.

TARTAKOVSKY, D. M. & WINTER, C. L. 2008 Uncertain future of hydrogeology. *ASCE J. Hydrol. Engrg* **13** (1), 37–39.

TREFRY, M. G., RUAN, F. P. & MCLAUGHLIN, D. 2003 Numerical simulations of preasymptotic transport in heterogeneous porous media: departures from the Gaussian limit. *Water Resour. Res.* **39**, 1063.

WHITE, B. L. & NEPF, H. M. 2003 Scalar transport in random cylinder arrays at moderate Reynolds number. *J. Fluid Mech.* **487**, 43–79.